JOURNAL OF PROPULSION AND POWER
Vol. 24, No. 3, May–June 2008

Burning Rate Characteristics of Ammonium Perchlorate-Based Composite Propellant Using Bimodal Ammonium Perchlorate

Makoto Kohga*
National Defense Academy,
Yokosuka, Kanagawa 239-8686, Japan

DOI: 10.2514/1.27107

It is well known that the burning rate of the ammonium perchlorate-based composite propellant depends on the mean particle diameter of ammonium perchlorate. Recently, it was reported that the packing fraction of ammonium perchlorate in the propellant matrix influences the burning rate. The mean particle diameter of the bimodal ammonium perchlorate system decreases by increasing the fine ammonium perchlorate content, and the packing fraction is a maximum when the coarse ammonium perchlorate content is approximately 0.8. The detailed experimental data on the burning rate characteristics of the propellants with bimodal ammonium perchlorate systems were investigated in this study. The burning rates of the ammonium perchlorate-based propellants at a constant mean diameter would not be identical when the packing fractions of the ammonium perchlorate particles were not constant. The burning rate of the bimodal ammonium perchlorate propellant is influenced not only by the mean particle diameter of the ammonium perchlorate, but also by the coarse ammonium perchlorate content and the diameter ratio of the coarse ammonium perchlorate to the fine ammonium perchlorate. The coarse ammonium perchlorate particles play an important role in the combustion of the bimodal ammonium perchlorate propellant even when the coarse particles are loosely dispersed in the fill region consisting of the fine particles and hydroxyl terminated polybutadiene. The combustion characteristics of the coarse ammonium perchlorate particles and the fill region would be the dominant factors influencing the burning rate of the bimodal ammonium perchlorate propellant.

Nomenclature

D	=	weight mean diameter, μm
D_c	=	weight mean diameter of coarse AP, μm
D_f	=	weight mean diameter of fine AP, μm
ξ_c	=	coarse AP content in bimodal AP
$\xi_{c,\text{prop}}$	=	coarse AP content of propellant prepared with monomodal AP
$\xi_{f,\text{fill}}$	=	fine AP content of fill region
$\xi_{f,\text{prop}}$	=	fine AP content of propellant prepared with monomodal AP

I. Introduction

AMMONIUM perchlorate (AP) is the most widely used oxidizer in composite propellants. The burning characteristics of the AP-based composite propellants have been studied and it has been reported that the combustion wave structure of AP-based propellants is heterogeneous because the physical structure of the propellants is heterogeneous [1–8]. However, the burning rate can be controlled by the physical properties of the combustion wave structure, such as the different sizes of the AP particles [7,9–12]. For example, it is generally known that the burning rate of propellants increases with the decreasing mean diameter of the AP particles. In the case of the constant AP content and pressure, the burning rate is quite dependent on D and represented by a smooth curve on a log–log graph [9,10].

Recently, it was reported that the burning rate of the AP-based propellant depends on the packing fraction of the AP particles, and some attempts were made to reveal the combustion mechanism of the AP-based propellant [12–15]. The D of the multimodal AP system can be calculated using the D of each AP sample and the mass fraction. However, the packing fraction of the multimodal AP system cannot be estimated from the packing fraction of each individual AP sample because the packing condition is dependent on various particle properties, such as particle diameter, size distribution, particle shape, adhesive and cohesive characters, etc. Especially, the AP particle has strong adhesive and cohesive properties.

The packing fraction of the fine AP particles is lower than that of the coarse particles. The packing fraction of the bimodal system can be superior to that of the monomodal system because the small particles fit in the interstitial spaces between the large particles. The maximum packing fraction would also be obtained at a particular value of the mass ratio: that of the coarse particle is approximately 0.8 [14,16]. On the other hand, D of the bimodal system decreases with the increasing mass fraction of the small particles. It would be expected that the burning rates of the AP-based propellants at a constant D would be nonidentical when the packing fractions of the AP particles were not constant. The objective of the present study is to obtain detailed experimental data on the burning rate characteristics of the AP-based propellants prepared with bimodal systems.

II. Experimental

The AP samples used in this study are shown in Table 1. Sample A was a commercial AP ground using a vibration ball mill for 5 min. Samples B–H were prepared by sifting commercial AP ground using a vibration ball mill. Sample I was prepared by the freeze–dry method [17]. Figure 1 shows scanning electron microscopy (SEM) photographs of AP samples A, B, E, and I. The D was measured using the SEM photographs. The D of the AP sample is shown in Table 1. Figure 2 shows the particle distribution of AP samples A, B, E, and G. Sample A has a wide distribution. The distributions of samples B–H are narrow because these are screened, and that of sample I is also narrow [17].

The propellant was prepared at 80% AP. Hydroxyl terminated polybutadiene (HTPB) was used as the binder. HTPB was cured with isophorone diisocyanate. Isophorone diisocyanate was added to 8% of the HTPB. The propellants prepared were designated by the

Presented as Paper 4924 at the 42nd AIAA/ASME/SAE/ASEE Joint Propulsion Conference and Exhibit, Sacramento, California, 9–12 July 2006; received 7 August 2006; revision received 30 July 2007; accepted for publication 3 August 2007.

*Associate Professor, Department of Applied Chemistry. Member AIAA.

Table 1 Monomodal AP samples used in this study

Symbol	Opening of sieve, μm Upper	Lower	D, μm
A	AP ground using vibration ball mill for 5 min		110
B	106	85	94
C	85	75	81
D	75	63	65
E	63	53	57
F	53	40	47
G	40	25	29
H	25	——	21
I	AP prepared by the freeze–dry method		3

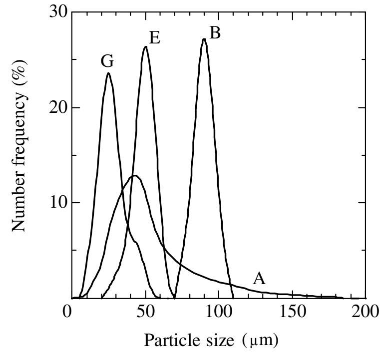

Fig. 2 Particle distribution of AP samples A, B, E, and G.

symbols of the AP sample. For example, the propellants prepared from sample A were designated as propellant A.

The size of each strand was 10 mm × 10 mm in cross section and 40 mm in length. The burning rate was measured in a chimney-type strand burner which was pressurized with nitrogen at 288 ± 2 K. The ignition of each strand was conducted by an electrically heated nichrome wire attached to the top of each strand. The burning rate was measured in a pressure range of 1–7 MPa, and was calculated with the cutoff period of two fuses which penetrate the strand at a 25 mm distance. The coefficient of variation of the burning rate was within ±5%.

The AP powder was densely packed in the 26.4 mm in diameter glass tube by tapping. The glass tube was tapped on a lauan board at a height of 10 mm. The sample weight was 10.00 g. The packing fraction was calculated under the closest packing condition.

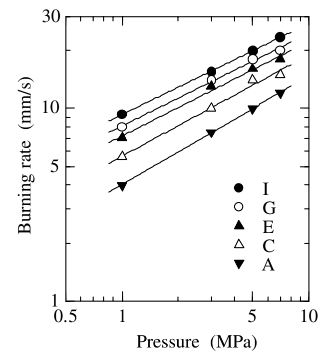

Fig. 3 Burning rate characteristics of monomodal AP propellants.

III. Results and Discussion

A. Burning Rate Characteristics of Propellant Prepared with Monomodal AP

Figure 3 shows the experimental data and corresponding fitting lines of the burning rate characteristics of propellants A, C, E, G, and I. The D of AP contained in the propellant decreased in alphabetical order as shown in Table 1. Their burning rates linearly increased on a logarithmic scale in the pressure range of 1–7 MPa. The burning rate increases with the decreasing D of the AP.

It is generally known that the burning rate of the AP/HTPB composite propellant is associated with the D of the AP [9,10]. The relationships between D and the burning rates at 1, 3, 5, and 7 MPa are shown in Fig. 4. At each pressure, the plots obtained in this study are also represented by a smooth curve in a similar manner to that described in previous papers [9,10].

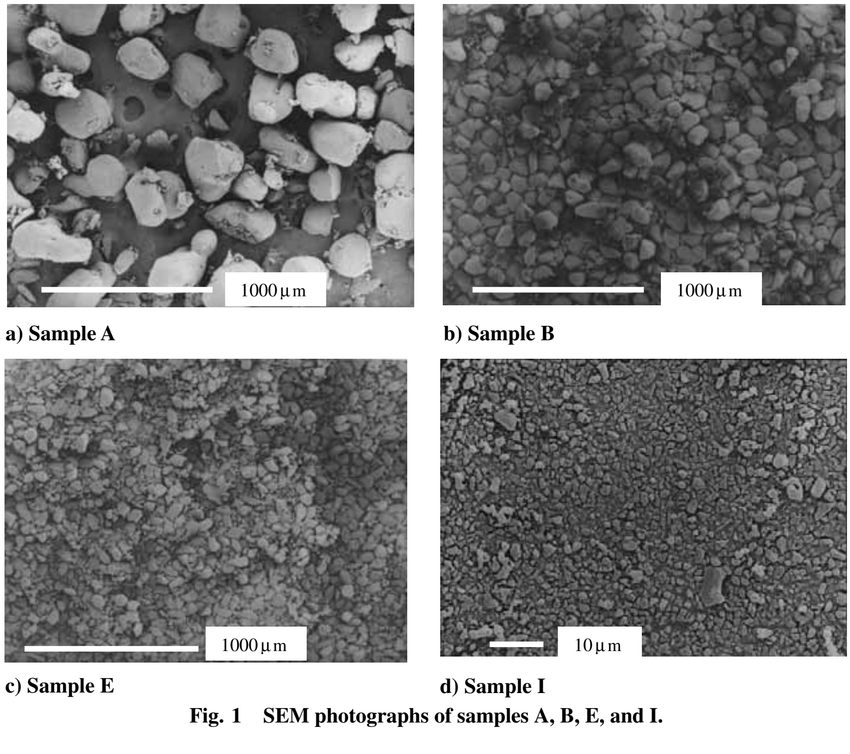

a) Sample A
b) Sample B
c) Sample E
d) Sample I

Fig. 1 SEM photographs of samples A, B, E, and I.

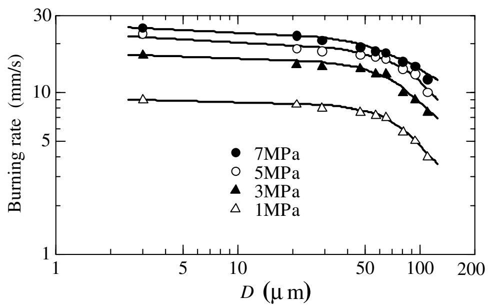

Fig. 4 Burning rate of monomodal AP propellants as a function of *D*.

B. Burning Rate Characteristics of Propellant Prepared with Bimodal AP

1. Comparison of Monomodal AP and Bimodal AP at Constant D

Bimodal AP samples were prepared as shown in Table 2. The *D* of the bimodal AP is 7, 17, 92, and 104 μm. The D_c/D_f of sample J-1 is the same as that of sample J-2. The D_c/D_f of sample J-4 is approximately 0.3 times that of samples J-1 and J-2, and the value of sample J-3 is equal to about 0.7 times that of sample J-4.

Figure 5 shows the burning rates of the propellants using these bimodal AP samples. The burning rates of a propellant prepared with the monomodal AP, of which the *D* is 7, 17, 92, and 104 μm, were determined on the basis of Fig. 4 and these are also plotted in Fig. 5. At 7 and 17 μm ($D_c/D_f = 7.0$), the burning rates above 3 MPa for the propellant containing the bimodal AP are slightly lower than those for the propellant incorporated with the monomodal AP. On the other hand, at 92 μm ($D_c/D_f = 1.7$) and 104 μm ($D_c/D_f = 2.3$), the burning rates of the propellant with the bimodal AP are almost the same as those of the propellant with the monomodal AP. These results indicate that the burning rate of the propellant using the bimodal AP with a large D_c/D_f would be lower than that of the propellant using the monomodal AP even when *D* is constant.

2. Bimodal AP with Constant D and Various Values of D_c/D_f

The bimodal AP samples with a constant *D* and various values of D_c/D_f were prepared to investigate the influence of D_c/D_f on the burning rate characteristics. The particle properties of the bimodal AP are shown in Table 3. The *D* of the bimodal AP is 94, 65, and 57 μm. These values of the bimodal samples are identical to those of the monomodal samples B, D, and E. The D_c/D_f is in the range of 1.9–36.7 and ξ_c is within the range of 0.159–0.850. Figure 6 illustrates the burning rate characteristics of these propellants using the bimodal AP as shown in Table 3. The burning rates of the propellant using the bimodal AP are definitely lower than those of the propellant using the monomodal AP in spite of the constant *D*.

At 57 and 65 μm, the burning rate decreases with the increasing D_c/D_f. The burning rate of the propellant using the bimodal AP with 94 μm decreases with the increasing D_c/D_f below 2.3. The burning rate at the D_c/D_f of 3.8 (K-2) is almost the same as that at the D_c/D_f of 2.3 (K-3), and the burning rate at 36.7 (K-1) is higher than that at 3.8 (K-2). These results indicate that the difference in the burning rate between the bimodal AP propellant and the monomodal AP propellant appears even at the small D_c/D_f ratio of 1.9, and the burning rate of the bimodal AP propellant does not always decrease with the increasing value of D_c/D_f. The ξ_c values of the propellants at 94 μm are larger than those of the propellants at 57 and 65 μm. These results suggest that the difference in the burning rate between the monomodal AP propellant and the bimodal AP propellant would be influenced by ξ_c, as well as D_c/D_f.

Table 2 Bimodal AP samples

Symbol	D_c, μm / D_f, μm	D_c/D_f, –	ξ_c, –	D, μm
J-1	21 / 3	7.0	0.200	7
J-2	21 / 3	7.0	0.800	17
J-3	110 / 67	1.7	0.600	92
J-4	110 / 47	2.3	0.900	104

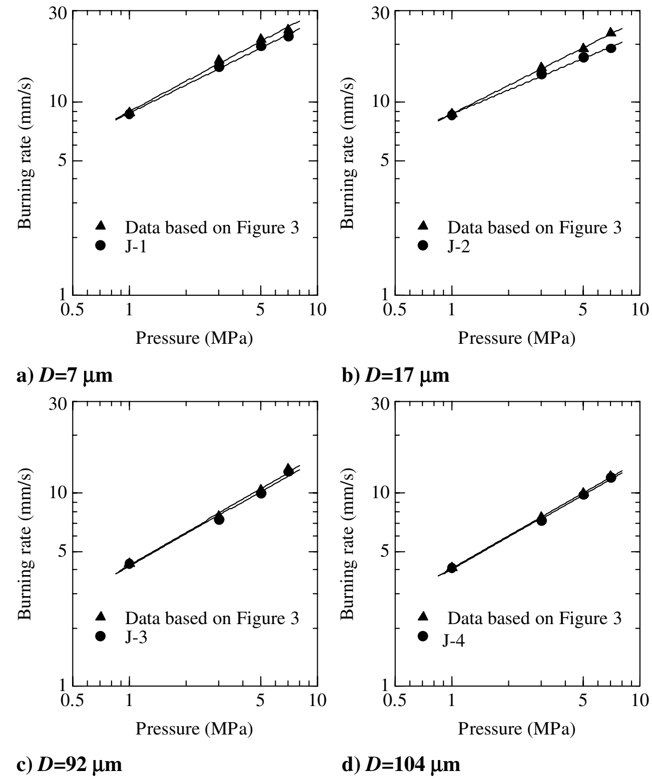

Fig. 5 Burning rate characteristics of propellant using bimodal AP.

Table 3 Bimodal AP with constant *D* and various values of D_c/D_f

Symbol	D_c, μm / D_f, μm	D_c/D_f, –	ξ_c, –	D, μm
K-1	110 / 3	36.7	0.850	94
K-2	110 / 29	3.8	0.803	
K-3	110 / 47	2.3	0.746	
K-4	110 / 57	1.9	0.699	
L-1	110 / 3	36.7	0.580	65
L-2	110 / 29	3.8	0.445	
L-3	110 / 47	2.3	0.286	
M-1	110 / 3	36.7	0.504	57
M-2	110 / 29	3.8	0.346	
M-3	110 / 47	2.3	0.159	

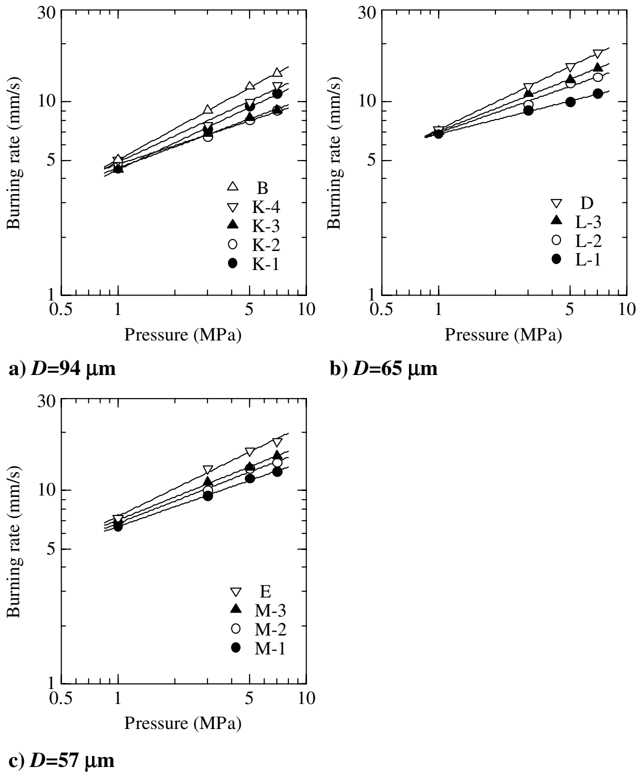

Fig. 6 Burning rate characteristics of propellant using bimodal AP with constant *D* and various values of D_c/D_f.

3. Bimodal AP with Constant D_c/D_f and Various Values of ξ_c

The bimodal AP samples with a constant D_c/D_f and various values of ξ_c were prepared to investigate the influence of ξ_c on the burning rate characteristics. The particle properties of the bimodal AP are shown in Table 4. Six monomodal samples, of which the *D* values are 3, 29, 47, 65, 94, and 110 μm, were used. The D_c/D_f is in the range of 1.2–36.7. The values of ξ_c are 0.800, 0.600, 0.400, and 0.200. Figure 7 shows the burning rate characteristics of these propellants prepared with the bimodal AP as shown in Table 4. For each propellant, these burning rates linearly increase on a logarithmic scale with the increasing pressure and decrease as ξ_c increases.

Table 4 Bimodal AP with constant D_c/D_f and various values of ξ_c

Symbol	D_c, μm / D_f, μm	D_c/D_f, –	ξ_c, –	D, μm
N-1			0.800	89
N-2	110 / 3	36.7	0.600	67
N-3			0.400	46
N-4			0.200	24
O-1			0.800	94
O-2	110 / 29	3.8	0.600	78
O-3			0.400	61
O-4			0.200	45
P-1			0.800	97
P-2	110 / 47	2.3	0.600	85
P-3			0.400	72
P-4			0.200	60
Q-1			0.800	101
Q-2	110 / 65	1.7	0.600	92
Q-3			0.400	83
Q-4			0.200	74
R-1			0.800	107
R-2	110 / 94	1.2	0.600	104
R-3			0.400	100
R-4			0.200	97

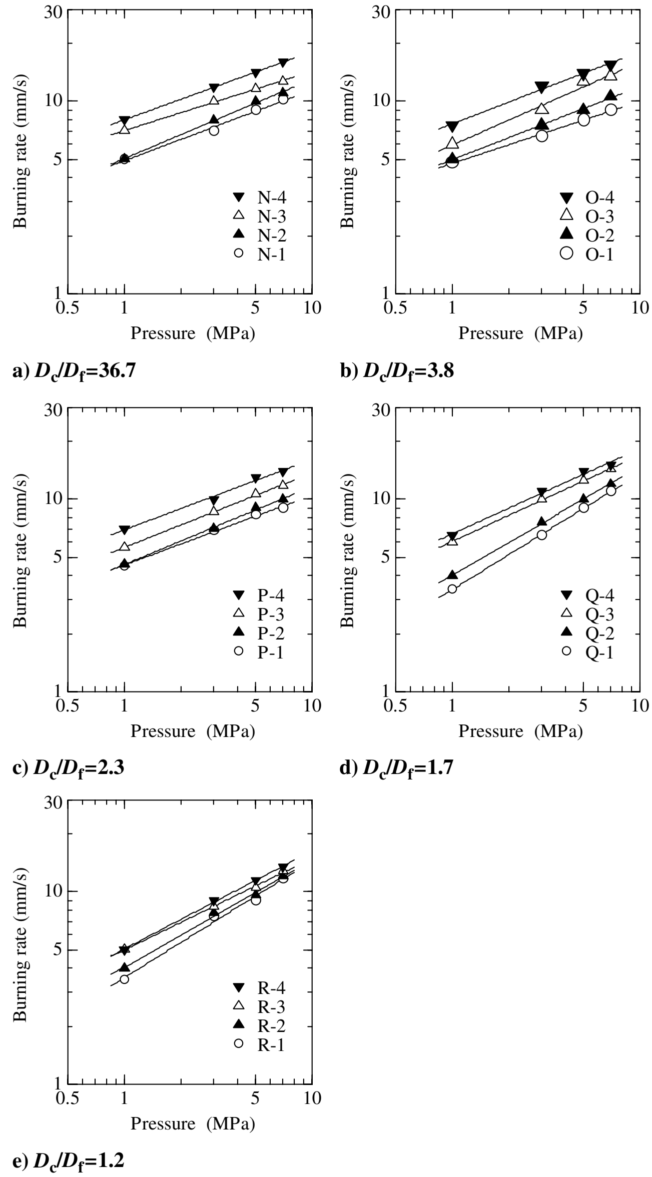

Fig. 7 Burning rate characteristics of propellant using bimodal AP with constant D_c/D_f and various values of ξ_c.

The relationships between ξ_c and the burning rates at 1, 3, 5, and 7 MPa are shown in Fig. 8. The burning rates of the propellants prepared at the ξ_c of 0 and 1, that is, the propellants using the monomodal AP, are plotted on the basis of Fig. 3. The burning rate at 1 MPa decreases with the increasing ξ_c. The burning rates at 3, 5, and 7 MPa decrease below the ξ_c of 0.8, and above that, increase as ξ_c increases.

A straight line is joined between the points at ξ_c of 0 and 1 at each pressure. If ξ_c was a dominant factor for the burning rate of the bimodal AP propellant, then the burning rate would be on this straight line. At 1.7, 2.3, 3.8, and 36.7 D_c/D_f, the burning rates at 1 MPa are nearly on the straight line. However the plots are below the lines at 3, 5, and 7 MPa. At the D_c/D_f of 1.2, the burning rates at both 1 and 3 MPa are approximately on each straight line and the plots are slightly below the lines at 5 and 7 MPa. These results suggested that ξ_c would be one of the important factors affecting the burning rate, but it would not be dominant.

The gap between the experimental data and the line decreases with the decreasing D_c/D_f. A lower D_c/D_f value indicates that the particle distribution is closer to monomodal. Therefore, the difference in the burning rate approaches zero and the influence of ξ_c

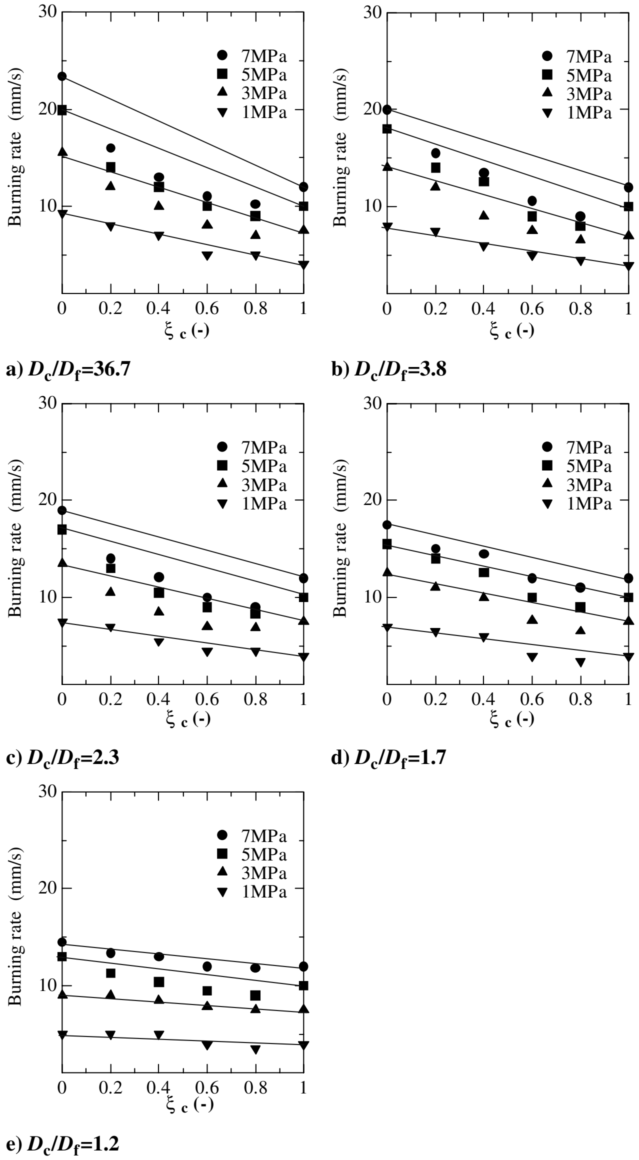

Fig. 8 Relationship between burning rate and ξ_c.

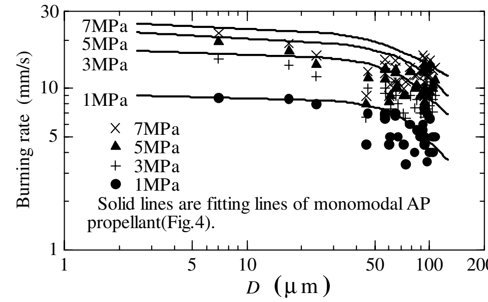

Fig. 9 Burning rate of bimodal AP propellants as a function of *D*.

on the burning rate becomes weaker as D_c/D_f decreases. It was found that the burning rate of the bimodal AP propellant would be influenced by D_c/D_f, ξ_c, and the pressure.

4. *Relationship Between Burning Rate and D of Bimodal AP Propellant*

The burning rate of the monomodal AP propellant is significantly dependent on D as described in Sec. III.A, and the burning rate of the bimodal AP propellant does not always agree with that of the monomodal AP propellant at a constant D as already mentioned. Figure 9 shows the relationship between the burning rate and D of the bimodal AP propellant. The burning rate decreases with the increasing D and the plots widely vary above 50 μm. The burning rate of the bimodal AP propellant is not apparently dependent on D, such as that of the monomodal AP propellant. The fitting lines of the monomodal AP propellant as shown in Fig. 4 are illustrated by the solid lines in Fig. 9. Most of the plots of the bimodal AP propellants are below the fitting lines of the monomodal AP propellant.

5. *Propellant Matrix*

The AP-based composite propellant prepared in this study consists of AP and HTPB. A cross-sectional view of the propellant was observed using SEM photographs to investigate the packing condition of the AP powder in the propellant matrix. Figure 10 shows the cross-sectional views of the propellants prepared at the ξ_c values of 0.200 and 0.800 for the bimodal AP propellants at the D_c/D_f ratio of 36.7. Some AP particles were likely to come off by cutting, but the observation of the propellant surface was not obstructed by this separation of the AP particles and binder.

A photograph of the propellant prepared at the ξ_c of 0.200 indicates that the fine AP particles are densely filled in the HTPB and the coarse AP particles are loosely dispersed in the fill region, consisting of the fine AP particles and HTPB. There were few agglomerates in the propellant matrix and most of the AP particles were dispersed in the HTPB. The mass of a 110 μm AP particle corresponds to approximately 5×10^4 particles of 3 μm AP. There are theoretically 2×10^5 particles of 110 μm AP and 4×10^{10} particles of 3 μm AP in a cubic centimeter of the propellant at the ξ_c of 0.200. The amount of the fine particles is 2×10^5 times as many as that of the coarse particles. These support the result from the cross-sectional view of the propellant. On the other hand, according to the photograph of the propellant surface at the ξ_c of 0.800, coarse AP particles are closely dispersed, compared to that at the ξ_c of 0.200, and the 3 μm AP particles are loosely scattered in HTPB. These photographs showed that there was a fill region composed of fine AP particles and HTPB. Furthermore, it was recognized that the coarse particles were dispersed in the fill region because the coarse particles are much bigger than the fine AP.

Figure 11 shows SEM photographs of the cross-sectional view of the bimodal AP propellant prepared with 94 μm and 110 μm APs at the ξ_c of 0.600 (R-2) and the monomodal AP propellant with 110 μm AP. The 110 μm and 94 μm particles were not distinguished on the surface of the bimodal AP propellant due to the small D_c/D_f. The cross-sectional view of this bimodal AP propellant was almost identical to that of the monomodal AP propellant.

6. *Combustion Mechanism of Bimodal AP Propellant*

The most remarkable feature of ξ_c and pressure on the burning rate of the bimodal AP propellant was obtained at the D_c/D_f ratio of 36.7 as described in Sec. III.B.3. The combustion mechanism of the bimodal AP propellant was discussed with the propellant prepared at the D_c/D_f of 36.7 in this section. As mentioned in the previous section, it would be presumed that the bimodal AP propellant at the D_c/D_f of 36.7 consisted of the coarse AP particles of 110 μm and the fill region, consisting of 3 μm AP particles and HTPB.

For the propellant prepared at the ξ_c of 0.200, the coarse AP particles are loosely dispersed in the fill region from Fig. 10a. The burning characteristics of the fill region would influence the burning rate of the bimodal AP propellant at the ξ_c of 0.200. The values of $\xi_{f,\mathrm{fill}}$ of the propellant at 0.200, 0.400, 0.600, and 0.800 ξ_c correspond to 0.762, 0.706, 0.615, and 0.444, respectively. The $\xi_{f,\mathrm{fill}}$ decreases with the increasing ξ_c.

The fill region consisted of 3 μm AP particles and HTPB. The burning rates of the monomodal AP propellant using the 3 μm AP at various AP contents were measured to investigate the burning characteristics of the fill region. In contrast, the burning rates of the monomodal AP propellant using the 110 μm AP were investigated. Figure 12 shows their burning rate characteristics. The burning rate decreases with the decreasing AP content. For the propellant with 3 μm AP, the propellants containing above the $\xi_{f,\mathrm{prop}}$ of 0.69 combust between 1 and 7 MPa. The propellant at the $\xi_{f,\mathrm{prop}}$ of 0.68

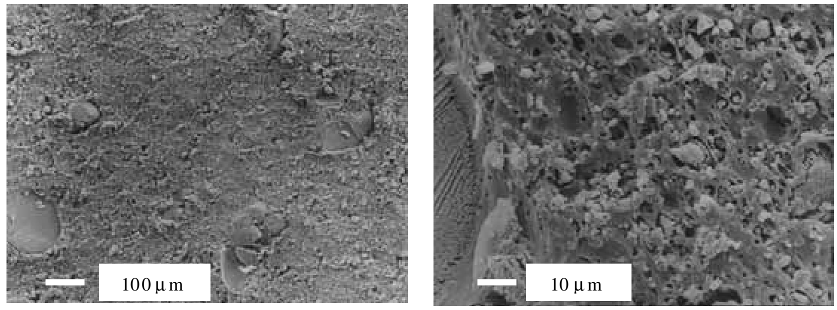

a) Propellant prepared at ξ_c of 0.200

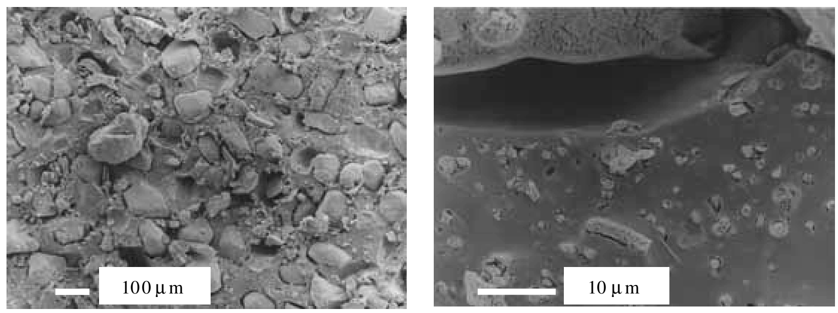

b) Propellant prepared at ξ_c of 0.800

Fig. 10 Cross-sectional view of bimodal AP propellant prepared at D_c/D_f of 36.7.

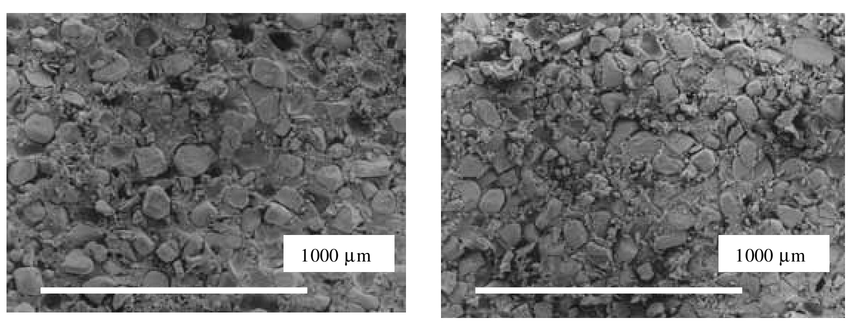

a) Bimodal AP propellant prepared with 94 μm and 110 μm AP at ξ_c of 0.600

b) Monomodal AP propellant prepared with 110 μm AP

Fig. 11 Cross-sectional view of bimodal AP propellant and monomodal propellant.

self-quenches at 7 MPa. The combustible pressure range decreases with the decreasing $\xi_{f,\text{prop}}$. The propellant at the $\xi_{f,\text{prop}}$ of 0.63 combusts only between 2 and 3 MPa, and the propellant at the $\xi_{f,\text{prop}}$ of 0.62 does not combust in the pressure range. For the propellant with 110 μm AP, the propellants containing above the $\xi_{c,\text{prop}}$ of 0.64 combust between 1 and 7 MPa. The propellant at the $\xi_{c,\text{prop}}$ of 0.62 self-quenches at 1 MPa and above 5 MPa. The combustible pressure range decreases with the decreasing $\xi_{c,\text{prop}}$ and the propellant at the $\xi_{c,\text{prop}}$ of 0.54 does not combust in this pressure range. The mechanism of the self-quenched combustion is reported in [18].

To clarify the effect of the AP content on the burning rate, the relationships between the AP content and the burning rates at 1, 3, 5, and 7 MPa are graphically illustrated in Fig. 13. The burning rate increases with the increasing AP content. The change in the burning rate increases as the AP content and pressure increase, especially when approaching the AP content of 0.80. This change in the burning rate of the propellant prepared with 3 μm AP is much greater than that of the propellant with the 110 μm AP. These results indicate that the influence of the AP content on the burning rate is remarkable at the higher pressure and higher AP content and, furthermore, this effect of the fine AP is more conspicuous than that of the coarse AP.

The increment of ξ_c indicates the increase in the content of the coarse AP contained in the bimodal AP propellant, that is, the value of $\xi_{f,\text{fill}}$ decreases. As ξ_c increases, the burning rate of the fill region decreases due to the decrease in $\xi_{f,\text{fill}}$. Table 5 shows the burning rate characteristics of the propellants prepared with the 3 and 110 μm APs. The values of $\xi_{f,\text{fill}}$ of the propellant at 0.200, 0.400, 0.600, and

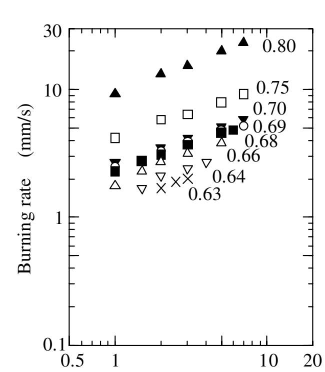

a) D=3 μm

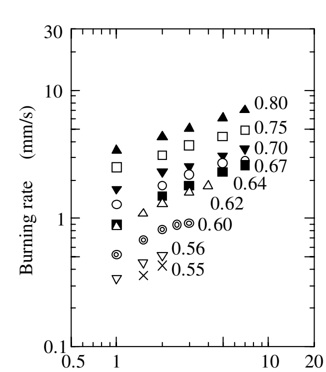

b) D=110 μm AP

Fig. 12 Burning rate characteristics of monomodal AP propellants using 3 μm AP and 110 μm AP.

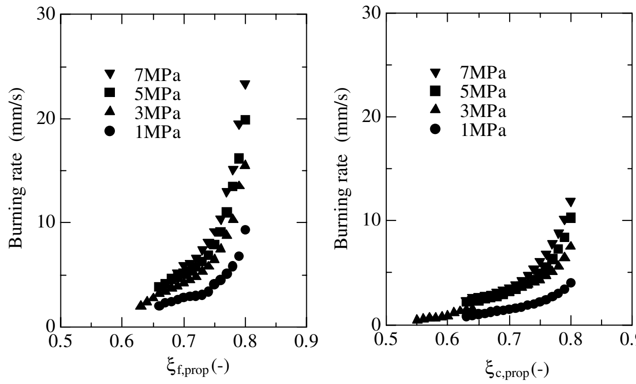

a) D=3 μm   b) D=110 μm

Fig. 13 Relationship between burning rate and AP content.

0.800 ξ_c correspond to 0.762, 0.706, 0.615, and 0.444, respectively. The burning rates of the fill regions at 0.762, 0.706, 0.615, and 0.444 $\xi_{f,\text{fill}}$ are identical with those of the monomodal AP propellant at 0.762, 0.706, 0.615, and 0.444 $\xi_{f,\text{prop}}$, respectively. According to Figs. 12a and 13a, the propellants at the $\xi_{f,\text{prop}}$ of 0.615 and 0.444 did not sustain the self-combustion due to the low AP content. The burning rates of the propellants prepared at the $\xi_{f,\text{prop}}$ of 0.762 and 0.706 are shown in Table 6. The burning rates of the bimodal AP propellants at the ξ_c values of 0.400 and 0.200 (N-3 and N-4) are higher than those of the monomodal AP propellants at the $\xi_{f,\text{prop}}$ values of 0.762 and 0.706, respectively. The coarse AP particles are loosely dispersed in the fill region according to the cross-sectional photograph of the propellant at the ξ_c of 0.200 (Fig. 10a). The lowering of the burning rate due to the decrease in $\xi_{f,\text{fill}}$ would be improved by the combustion of the coarse AP particles in the fill region even when the coarse AP particles are loosely dispersed. It was found that the coarse AP particles would have an important role in the combustion of the bimodal AP propellant.

As shown in Fig. 13, the burning rate of the propellant prepared with the 3 μm AP is higher than that of the propellant with the 110 μm AP at the constant AP content, and the change in the burning rate versus the AP content at higher pressures is greater than that at lower pressures. This tendency of the propellant prepared with the fine AP is more conspicuous than that of the propellant with the coarse AP. These results indicate that the decrease in the burning rate due to the decrease in $\xi_{f,\text{fill}}$ would not be entirely compensated by the increase in the burning rate due to the increase in the coarse AP content, though the decrease in the fine AP content equals the increase in the coarse AP content. Therefore, the burning rates of the bimodal AP propellant would be below the straight lines as indicated in Fig. 8. The gap between the straight line and the burning rate at the higher pressure would be greater than that at the lower pressure because the increase in the burning rate due to the change in the coarse AP content would not be able to compensate for the decrease in the burning rate due to the decrease in $\xi_{f,\text{fill}}$ especially at higher pressures.

It is generally known that the burning rate of the AP-based composite propellant increases with the decreasing particle diameter. Even though these propellants (N-1 and N-2) at the ξ_c values of 0.600 and 0.800 contained fine AP particles, the burning rates at 5 and 7 MPa of these propellants are lower than those at the propellant at the ξ_c of 1, that is, the monomodal AP propellant with 110 μm AP. The $\xi_{f,\text{fill}}$ of the propellants at 0.600 and 0.800 ξ_c values are 0.615 and 0.444, respectively. These fill regions did not sustain self-combustion according to Fig. 12a. Therefore, the burning rates of the propellants at the 0.600 and 0.800 ξ_c values would be presumably lower than those at the ξ_c of 1.

The coarse AP contents of the propellants at the ξ_c values of 0.600 and 0.800 are 0.706 and 0.762 when the fine AP is neglected. The propellants at 0.706 and 0.762 $\xi_{c,\text{prop}}$ are capable of self-sustaining combustion according to Fig. 12b. The burning rates of the propellants at the $\xi_{c,\text{prop}}$ values of 0.762 and 0.706 are shown in Table 7. The burning rates of the bimodal AP propellants at the ξ_c values of 0.800 and 0.600 are higher than those of the monomodal AP propellants at the $\xi_{c,\text{prop}}$ values of 0.762 and 0.706, respectively. This is because the fine AP particles are dispersed in the fill regions of these bimodal AP propellants as shown in Fig. 10b and HTPB in these monomodal AP propellants at the $\xi_{c,\text{prop}}$ of 0.762 and 0.706 do not have the fine AP particles. The burning rate of the bimodal AP propellant would be improved by the fill region even when the fill region did not sustain self-combustion. The burning rate of the bimodal AP propellant would be influenced by the combustion characteristics of the coarse AP particles and the fill region.

For the bimodal AP propellants prepared with 1.2 D_c/D_f, the distinction between the 110 and 94 μm particles were not apparent at the propellant surface and the cross-sectional views of this bimodal AP propellant was almost the same as that of the monomodal AP propellant with 110 μm AP as shown in Fig. 11. Because the influence of D_c/D_f on the burning rate decreased with the decreasing D_c/D_f ratio, the burning rate of the bimodal AP propellant would be close to the straight lines as shown in Fig. 8.

C. Packing Condition of AP Powder

The burning rate of the propellant at 7 MPa using the bimodal AP with the 36.7 D_c/D_f ratio has the most conspicuous influence of ξ_c on the burning rate characteristics in Fig. 8. The burning rate at 7 MPa decreases with the increasing ξ_c and reaches a minimum at the ξ_c of 0.800. The packing fraction of the AP powder is significantly dependent on D_c/D_f and the mass ratio of the coarse particles to fine particles, and the largest packing fraction is obtained at the mass ratio of the coarse particles in the range of 0.75 to 0.80 [14,16]. This relationship between the burning rate and ξ_c was similar to that between the packing fraction and the mass ratio of the coarse particles.

The packing fraction at the closest condition of the bimodal AP shown in Table 4 was measured by the tapping method. Figure 14 shows the packing fraction of the bimodal AP. The largest packing

Table 5 Burning rate characteristics of propellants prepared with 3 μm AP and 110 μm AP

			Burning rate, mm/s			
Symbol	ξ_c, −	$\xi_{f,\text{fill}}$, −	1 MPa	3 MPa	5 MPa	7 MPa
A	1.0	0.0	4.0	7.4	10.3	11.9
N-1	0.800	0.444	4.9	7.0	9.1	10.2
N-2	0.600	0.615	5.1	7.9	9.9	11.1
N-3	0.400	0.706	7.1	10.0	11.6	12.7
N-4	0.200	0.762	8.0	11.9	14.1	16.0
I	0.0	0.800	9.3	15.5	19.9	23.4

Table 6 Burning rate characteristics of monomodal AP propellant prepared with 3 μm AP

	Burning rate, mm/s			
$\xi_{f,\text{prop}}$, −	1 MPa	3 MPa	5 MPa	7 MPa
0.706	2.9	4.5	5.4	6.1
0.762	4.5	7.4	9.1	10.4

Table 7 Burning rate characteristics of monomodal AP propellant prepared with 110 μm AP

	Burning rate, mm/s			
$\xi_{c,\text{prop}}$, −	1 MPa	3 MPa	5 MPa	7 MPa
0.706	1.6	2.8	3.4	3.9
0.762	2.4	4.5	5.5	6.8

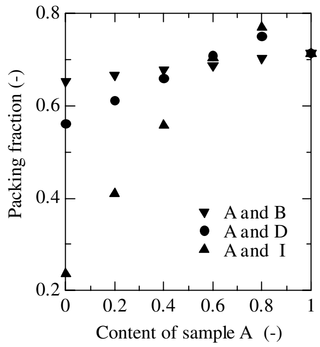

Fig. 14 Packing fraction of bimodal AP.

fraction was not remarkably obtained at the coarse AP content of 0.8 and the bimodal AP system of the 110 and 3 μm AP particles did not have a maximum. The AP packing layer had a large amount of void space. This is because the fine AP particles have a strong adhesive property and would agglomerate. The agglomerates were few in the propellant matrix and most of the AP particles were dispersed in HTPB as described in Sec. III.B.5. It was found that the packing by tapping did not represent the condition of the AP particles dispersed in the propellant matrix.

IV. Conclusions

The detailed experimental data on the burning rate characteristics of the AP-based propellants prepared using bimodal systems were investigated in this study. The burning rate of the AP/HTPB composite propellant with the monomodal AP is associated with the weight mean diameter of AP. On the other hand, the burning rate of the propellant with the bimodal AP propellant is influenced not only by the mean particle diameter of AP, but also by the coarse AP content and the diameter ratio of the coarse AP to fine AP. The burning rate of the bimodal AP propellant is not always equal to that of the monomodal AP propellant at a constant mean particle diameter. The difference in the burning rate between the bimodal AP propellant and the monomodal AP propellant increases with the increasing pressure and diameter ratio. The burning rates of some bimodal AP propellants are lower than those at the monomodal AP propellant with the coarse AP even though the bimodal AP propellants contain fine AP particles. The burning rate of the bimodal AP propellant was a minimum value around the coarse AP content of 0.8. The coarse AP particles had an important role in the combustion of the bimodal AP propellant even when the coarse particles are loosely dispersed in the fill region consisting of fine particles and HTPB. The burning rate of the bimodal AP propellant would be influenced by the combustion characteristics of the coarse AP particles and the fill region.

References

[1] Boggs, T. L., Derr, R. L., and Beackstead, M. W., "Surface Structure of Ammonium Perchlorate Composite Propellants," *AIAA Journal*, Vol. 8, No. 2, 1970, pp. 370–372.

[2] Ramohalli, K. N. R., "Steady-State Burning of Composite Propellants Under Zero Cross-Flow Situations," *Fundamentals of Solid-Propellant Combustion*, edited by K. K. Kuo, and M. Summerfield, Vol. 90, Progress in Astronautics and Aeronautics, AIAA, New York, 1984, pp. 409–477.

[3] Kubota, N., Kuwahara, T., Miyazaki, S., Uchiyama, K., and Hirata, N., "Combustion Wave Structures of Ammonium Perchlorate Composite Propellants," *Journal of Propulsion and Power*, Vol. 2, No. 4, 1986, pp. 296–300.

[4] Kubota, N., "Flame Structure of Modern Solid Propellants," *Nonsteady Burning and Combustion Steability of Solid Propellants*, edited by L. D. Luca, E. W. Price, and M. Summerfield, Vol. 143, Progress in Astronautics and Aeronautics, AIAA, New York, 1992, pp. 233–260.

[5] Beackstead, M. W., "Solid Propellant Combustion Mechanisms and Flame Structure," *Pure and Applied Chemistry*, Vol. 65, No. 2, 1993, pp. 297–307.
doi:10.1351/pac199365020297

[6] Bilger, R. W., Jia, X., Li, J. D., and Nguyen, T. T., "Theoretical and Experimental Study of Composite Solid Propellant Combustion," *Combustion Science and Technology*, Vol. 115, No. 1, 1996, pp. 1–39.
doi:10.1080/00102209608935521

[7] Al-Harthi, A., and Williams, A., "Effect of Fuel Binder and Oxidizer Particle Diameter on the Combustion of Ammonium Perchlorate Based Propellants," *Fuel*, Vol. 77, No. 13, 1998, pp. 1451–1468.
doi:10.1016/S0016-2361(98)00059-3

[8] Charkravarthy, S. R., Seizman, J. M., Price, E. W., and Sigman, R. K., "Intermittent Burning of Ammonium Perchlorate-Hydrocarbon Binder Monomodal Matrixes, Sandwiches, and Propellants," *Journal of Propulsion and Power*, Vol. 20, No. 1, 2004, pp. 101–109.

[9] Bastress, E. Karl, "Modification of the Burning Rates of Ammonium Perchlorate Solid Propellants by Particle Size Control," Ph.D. Dissertation, Aeronautical Engineering, Princeton Univ., Princeton, NJ, 1961.

[10] Tsujikado, N., Ohyumi, Y., Ohmura, I., Harada, T., and Aboshi, M., "Burning Rate Control of HTPB Propellants," *Kayaku Gakkaishi*, Vol. 41, No. 5, 1980, pp. 287–292.

[11] Bozic, V. S., and Milos, M. V., "Effects of Oxidizer Particle Size on Propellants Based on Modified Polyvinyl Chloride," *Journal of Propulsion and Power*, Vol. 17, No. 5, 2001, pp. 1012–1016.

[12] Jackson, T. L., and Buckmaster, J., "Heterogeneous Propellant Combustion," *AIAA Journal*, Vol. 40, No. 6, 2002, pp. 1122–1130.

[13] Kochevets, S., Buckmaster, J., Jackson, T. L., and Hegab, A., "Random Packs and Their Use in Modeling Heterogeneous Solid Propellant Combustion," *Journal of Propulsion and Power*, Vol. 17, No. 4, 2001, pp. 883–891.

[14] Knott, G. M., Jackson, T. L., and Buckmaster, J., "Random Packing of Heterogeneous Propellants," *AIAA Journal*, Vol. 39, No. 4, 2001, pp. 678–686.

[15] Massa, L., Jackson, T. L., and Buckmaster, J., "New Kinetics for a Model of Heterogeneous Propellant Combustion," *Journal of Propulsion and Power*, Vol. 21, No. 5, 2005, pp. 914–924.

[16] Hagihara, Y., "Paking of Ammonium Perchlorate Particles by Tapping (1) Bimodal Systemt," *Kogyo Kayaku*, Vol. 44, No. 6, 1983, pp. 347–351.

[17] Kohga, M., and Hagihara, Y., "Preparation of Fine Ammonium Perchlorate by Freeze-Drying," *Kagaku Kougaku Ronbunshu*, Vol. 23, No. 2, 1997, pp. 163–169.

[18] Kohga, M., and Hagihara, Y., "Self-Quenched Combustion of Fuel-Rich AP/HTPB Composite Propellant," *Science and Technology of Energetic Materials*, Vol. 64, No. 2, 2003, pp. 68–74.

S. Son
Associate Editor